Bile Acid Sequestration by Colesevelam Reduces Bile Acid Hydrophobicity and Improves Liver Pathology in *Cyp2c70*$^{-/-}$ Mice with a Human-Like Bile Acid Composition

Anna Palmiotti , Hilde D. De Vries , Milaine V. Hovingh , Martijn Koehorst , Niels L. Mulder , Esther Verkade , Melany K. Veentjer , Theo H. Van Dijk , Vincent W. Bloks , Rick Havinga , Henkjan J. Verkade , Jan Freark De Boer * , Folkert Kuipers *

Posted Date: 10 August 2023

doi: 10.20944/preprints202308.0779.v1

Keywords: bile acids; colesevelam; enterohepatic circulation; liver; humanized mouse model

Article

Bile Acid Sequestration by Colesevelam Reduces Bile Acid Hydrophobicity and Improves Liver Pathology in *Cyp2c70*$^{-/-}$ Mice with a Human-Like Bile Acid Composition

Anna Palmiotti [1], Hilde D. de Vries [2], Milaine V. Hovingh [1], Martijn Koehorst [2], Niels L. Mulder [1], Esther Verkade [1], Melany K. Veentjer [1], Theo H. van Dijk [2], Vincent W. Bloks [1], Rick Havinga [1], Henkjan J. Verkade [1], Jan Freark de Boer [1,2,*] and Folkert Kuipers [1,3,*]

[1] Department of Pediatrics; University of Groningen, University Medical Center Groningen, 9713 GZ Groningen, The Netherlands; a.palmiotti@umcg.nl; m.v.hovingh@umcg.nl; n.l.mulder@umcg.nl; e.verkade@umcg.nl; v.w.bloks@umcg.nl; h.havinga@umcg.nl; h.j.verkade@umcg.nl; j.f.de.boer@umcg.nl; f.kuipers@umcg.nl

[2] Department of Laboratory Medicine; University of Groningen, University Medical Center Groningen, 9713 GZ Groningen, The Netherlands; h.d.de.vries@umcg.nl; j.f.de.boer@umcg.nl

[3] European Research Institute for the Biology of Ageing (ERIBA), University of Groningen, University Medical Center Groningen, 9713 GZ Groningen, The Netherlands; f.kuipers@umcg.nl

* Correspondence: Jan Freark de Boer, j.f.de.boer@umcg.nl; Tel.: +31 50 361 4865; Folkert Kuipers, f.kuipers@umcg.nl Tel.: +31 50 361 6620

Abstract: Bile acids (BAs) and their signalling pathways have been identified as therapeutic targets for liver and metabolic diseases. We generated *Cyp2c70*$^{-/-}$ (KO) mice that are not able to convert chenodeoxycholic acid into rodent-specific muricholic acids (MCAs) and, hence, possess a more hydrophobic, human-like BA pool. Recently, we have shown that KO mice display cholangiopathic features with development of liver fibrosis. The aim of this study was to determine whether BA sequestration modulates liver pathology in Western type-diet (WTD)-fed KO mice. The BA sequestrant colesevelam was mixed into the WTD (2% w/w) of male *Cyp2c70*$^{+/+}$ (WT) and KO mice and the effects were evaluated after 3 weeks of treatment. Colesevelam increased fecal BA excretion in WT and KO mice and reduced the hydrophobicity of biliary BAs in KO mice. Colesevelam ameliorated diet-induced hepatic steatosis in WT mice, whereas KO mice were resistant to diet-induced steatosis and BA sequestration had no additional effects on liver fat content. Total cholesterol concentrations in livers of colesevelam-treated WT and KO mice were significantly lower than those of untreated controls. Of particular note, colesevelam treatment normalized plasma levels of liver damage markers in KO mice and markedly decreased hepatic mRNA levels of fibrogenesis-related genes in KO mice. Lastly, colesevelam did not affect glucose excursions and insulin sensitivity in WT or KO mice. Our data show that BA sequestration ameliorates liver pathology in *Cyp2c70*$^{-/-}$ mice with a human-like bile acid composition without affecting insulin sensitivity.

Keywords: bile acids; colesevelam; enterohepatic circulation; liver; humanized mouse model

1. Introduction

Besides their classical function in absorption of dietary fat-soluble nutrients and vitamins, bile acids (BAs) have been identified as signalling molecules involved in the regulation of lipid, glucose, energy metabolism and modulation of immune responses [1]. Their action on metabolism is manifested through the activation of several intracellular nuclear receptors, such as the farnesoid X receptor (FXR/NR1H4), pregnane X receptor (PXR/NR1I2), vitamin D receptor (VDR) and the constitutive androstane receptor (CAR /NR1I3), as well as cell surface G protein–coupled receptors (GPCRs), such as the Takeda G protein–coupled receptor 5 (TGR5/GPBAR1). Due to their involvement in multiple metabolic pathways, BAs and their signalling pathways represent targets for therapeutic intervention in (metabolic) diseases. In fact, BAs have been used for many years to

 doi:10.20944/preprints202308.0779.v1

treat gallstones, cholestatic liver diseases [2] and currently ursodeoxycholic acid (UDCA) is part of the standard treatment for primary biliary cholangitis (PBC) [3]. Additionally, synthetic and natural modulators of FXR have been tested in animal models displaying liver inflammation, fibrosis and liver steatosis [4,5]. In addition, beneficial effects of pharmacological FXR stimulation have also been demonstrated in clinical trials: Obeticholic acid (OCA) treatment has been shown to exert positive effects in patients with primary biliary cholangitis (PBC) [6–8] and is now approved by the FDA and EMA for the treatment of PBC in patients that have an incomplete response or are intolerant to UDCA [9]. Furthermore, it is well-established that BA sequestrants, compounds that bind BAs in the intestine and thereby prevent their re-absorption, reduce plasma LDL cholesterol levels and cardiovascular diseases in patients with hyperlipidaemia by stimulating BA production and, thus, cholesterol catabolism [10]. Additionally, inhibiting intestinal BA re-absorption (either with BA sequestrants or by pharmacological ASBT inhibition) ameliorates BA-mediated cholestatic liver and bile duct injury in mouse models of cholestatic liver injury and sclerosing cholangitis [11,12]. Yet, studies have also indicated that the BA sequestrant colesevelam may lower plasma glucose levels as wells as HbA1c in patients with type 2 diabetes mellitus (T2DM) [13–15]. BA sequestration reduces plasma glucose levels in diabetic *db*/*db* mice by increasing the metabolic clearance rate in peripheral tissues [16]. Yet, the exact mechanism driving the improved glucose homeostasis upon BA sequestration remains to be elucidated. On the other hand, it has been reported that BA sequestration may increase VLDL-triglyceride (TG) production and results in moderately elevated plasma TG levels in humans [17,18]. The majority of preclinical studies that have provided the basis for current understanding of the impact of BAs and their signalling pathways on metabolism and liver function have been conducted in murine models. However, several differences in BA metabolism between mice and humans complicate the translation of murine experimental data to the human situation. In contrast to humans, mice metabolize chenodeoxycholic acid (CDCA) to muricholic acids (MCAs) in the liver, which is mediated by the mouse-/rat-specific enzyme CYP2C70. Therefore, hydrophilic and cytoprotective MCA species, which are poor agonists for FXR and TGR5, are highly abundant in the murine BA pool while the most potent physiological agonist of the FXR, hydrophobic and cytotoxic CDCA, is abundant in the human bile acid pool but only present in very low amounts in mice. To better translate murine data to the human situation, a mouse model with a human-like BA metabolism has been developed [19–21]. In this model the gene encoding CYP2C70 has been inactivated [19]. It has been reported that *Cyp2c70*$^{-/-}$ mice show elevated plasma bile acid and transaminase levels and develop hepatic fibrosis [19,22]. In this study, we aimed to investigate whereas BA sequestration impacts hepatic lipid accumulation and other liver-related pathological features in WTD-fed KO mice.

2. Materials and Methods

2.1. Animals

12 to 14-weeks old male *Cyp2c70*$^{-/-}$ (KO) mice (n=17) on a C57BL/6J background (C57BL/6J-Cyp2c70^{em3Umcg}) and wild-type (WT) littermates (n=18), bred at the local animal facility (CDP) of the University Medical Center Groningen, were housed individually in a temperature-controlled room (21°C) with a light/dark-cycle of 12 hours each. During the study, mice had ad libitum access to food and water. Mice were exposed to a Western type diet (WTD), containing 60% energy from fat and 0.25% added cholesterol (D14010701Bi, Research Diets Inc., New Brunswick, NJ, USA), for a period of 8 weeks prior to colesevelam intervention. Part of the mice (KO mice n=9, WT mice n=9) were subsequently treated with 2% (w/w) colesevelam hydrochloride (HCl) (182815-44-7 Daiichi Sankyo Pharma Development, Edison, NJ, USA., NJ 08837) mixed into the WTD, while the other part of the animals (KO mice n=8, WT mice n=9) remained on WTD without colesevelam as control. Body weight (BW) and food intake (FI) were monitored weekly. Body composition was analyzed after 2 weeks of colesevelam treatment. Oral glucose tolerance tests and insulin analysis were performed at 2 weeks after start of the colesevelam treatment. After 3 weeks of colesevelam treatment, under isoflurane anesthesia mice were euthanized through cardiac puncture followed by cervical dislocation. Plasma

 doi:10.20944/preprints202308.0779.v1

and organs were collected and stored at -80°C until analysis. Fecal samples were collected at the end of colesevelam treatment for 3 days prior to termination. All animal experiments were approved by the Dutch Central Committee for Animal Experiments and the Animal Welfare Body of the University of Groningen (Dutch National Central Commission for Animal Experiments, CCD, license number AVD10500202115290).

2.2. Body weight, food intake, and body composition analysis

To determine body weights and food intake, weekly measurements were made on individually housed animals. Using a Minispec Body Composition Analyzer (LF90-II, Bruker BioSpin GmbH, Rheinstetten, Germany), after 2 weeks of treatment, non-invasive measurements of body composition (fat mass, lean mass and fluid mass) were performed in conscious mice after 4 hours of fasting,

2.3. Assessment of glucose tolerance and insulin resistance

To examine glucose excursions, an oral glucose tolerance test (OGTT) was performed after 2 weeks of colesevelam treatment. After 4 hours of fasting (08:00-12:00h), mice received an oral glucose bolus (2 g/kg BW) by gavage. Using a portable glucose meter (Accu-Chek Performa, Roche Diabetes Care, Almere, The Nederlands), blood glucose levels were measured before and 5, 15, 30, 45, 60, 90, and 120 minutes after gavage. To explore the effect of administered glucose on insulin levels, blood spots were also taken before and at 5, 15, 60, and 120 minutes after gavage for insulin measurement, as previously described [23]. Blood spots were briefly air-dried and stored at -20ºC for insulin measurements (Crystal Chem rat insulin ELISA (#90010) with mouse insulin standard (#90020), Zaandam, The Netherlands). Plasma HOMA-IR index was calculated multiplying the fasting blood glucose levels by the fasting plasma insulin levels and dividing the product by 14,1 [24].

2.4. Plasma biochemistry

Plasma triglycerides (Roche Diagnostics, Rotkreuz, Switzerland) and total cholesterol (DiaSysDiagnostic Systems, Holzheim Germany) were measured utilizing commercially available reagents. Plasma levels of aspartate aminotransferase (AST), alanine aminotransferase (ALT) and albumin were quantified using routine clinical chemistry analyzer (Cobas 6000, Roche Diagnostics) with standard reagents (Roche Diagnostics).

2.5. Bile acid measurements

Plasma and gallbladder bile BA species were quantified by liquid chromatography–tandem mass spectrometry technique (LCMS) using a Nexera X2 Ultra High-Performance Liquid Chromatography system (SHIMADZU, Kyoto, Japan), linked to a SCIEX QTRAP 4500 MD triple quadrupole mass spectrometer (SCIEX, Framingham, MA, USA) (UHPLC-MS/MS) as previously described [25]. To quantify fecal BAs, individual mouse feces were collected for 72 hours, then desiccated and finely ground. About 30 mg of dried feces were incubated in 0.5 M sodium hydroxide (NaOH) and methanol (MeOH) at 80°C for 3 hours. The boiled feces were ultra-sonicated and centrifuged. Part of the supernatant was mixed with the internal standard, MeOH and 0,375 M hydrochloric acid (HCL). BAs were purified using Oasis HLB columns (Waters, Milford, MA, USA) rinsed with 0,25 M HCL solution and hexane. Samples were then dried at 50°C under a stream of nitrogen and dissolved in 50% MeOH for quantification by LCMS using 5ß-cholanic acid 7α,12α diol as internal standard.

2.6. Hepatic lipid analyses

After lipid extraction from homogenates as described by Bligh and Dyer [26], hepatic triglycerides, total cholesterol, and phospholipids were measured with commercially available reagents (systems from Roche Diagnostics and Diasys Diagnostic, respectively).

 doi:10.20944/preprints202308.0779.v1

2.7. Fecal neutral sterol analyses

For quantification of fecal neutral sterol excretion, individual mouse feces were collected for 72 hours, then desiccated and finely ground. About 50 mg of dried feces were incubated in alkaline methanol at 80°C for 2 hours. Neutral sterols were then extracted 3 times with petroleum ether (boiling range 60-80 0C) and derivatized with pyridine/ N,O-Bis (trimethylsilyl) trifluoroacetamide (BSTFA)/ trimethylchlorosilane (TMCS) (50:50:1) for 1 hour. Samples were then dried at room temperature under a stream of nitrogen and dissolved in heptane with 1% BSTFA to be quantified by GC using 5β-cholestane as internal standard [27].

2.8. Determination of mRNA levels

Total RNA was extracted from liver and distal small intestine utilizing TRI-reagent (Sigma, St. Louis, MO, USA), quantified utilizing NanoDrop (NanoDrop Technologies, Wilmington, DE, USA), and reverse transcribed utilizing Moloney–Murine Leukemia Virus reverse transcriptase (Life Technologies, Bleiswijk, The Netherlands). Total RNA from brown adipose tissue (BAT) was extracted with an RNeasy Lipid Tissue Mini Kit (QIAGEN Sciences, Maryland, United States) quantified by NanoDrop and reverse transcribed as described previously. Real-time quantitative PCR analyses were performed on a StepOnePlus™ Real-Time PCR system (Applied Biosystems, Foster City, CA, USA). Gene expression levels were normalized to Cyclophilin as a housekeeping gene for liver and intestine, and 36b4 (Rplp0) as a housekeeping gene for BAT and then further normalized to the respective control group's mean.

2.9. Histology and staining of liver

After termination, part of the liver tissue was quickly excised and fixed in 4% formalin for 24 hours prior to embedding in paraffin. Sections (4µm) were cut and stained with haematoxylin and eosin to determine liver morphology or Sirius Red/Fast Green to visualize collagen deposition. Immunohistochemical staining for cholangiocytes was performed using an anti-cytokeratin 19 (CK19) antibody (ab52625; Abcam, Cambridge, United Kingdom) in accordance with the manufacturer's guidelines. Images were obtained using a Hamamatsu NanoZoomer (Hamamatsu Photonics, Almere, The Netherlands).

2.10. Determination of fecal energy content and energy absorption

~300 mg of powdered dry feces samples were combusted in a Parr 6100 compensated calorimeter (Parr Instrument Company, Moline, IL, USA) with a 1108 Oxygen Bomb placed in 2000 g of demineralized water. The temperature increase of the water determined the caloric content of the feces. The intra-assay variability was ~0.3%. The energy absorption efficiency (%) was calculated as: (1-(energy loss/energy intake)) *100.

2.11. Statistical analysis

Results are presented as Tukey box-whisker plots or line graphs with mean and ±SD generated using GraphPad Prism (version 8, GraphPad Software, San Diego, CA). Significant differences in multiple group comparisons were determined by the Kruskal-Wallis H test, followed by Conover post-hoc comparisons in Brightstat [28]. Differences with a p-value $p<0.05$ were considered statistically significant.

3. Results

3.1. Colesevelam does not affect body weight of WTD-fed Cyp2c70$^{-/-}$ mice.

Twelve to 14-weeks old male Cyp2c70$^{+/+}$ (WT) and Cyp2c70$^{-/-}$ (KO) mice were fed a Western-type diet (WTD) for 8 weeks in order to induce obesity and insulin resistance. Prior to the start of the intervention, body weights and food intake of WT and KO were comparable during the 8 weeks of

Preprints (www.preprints.org) | NOT PEER-REVIEWED | Posted: 10 August 2023 doi:10.20944/preprints202308.0779.v1

WTD feeding (data not shown). Part of the mice were subsequently treated with colesevelam (2% w/w mixed into the WTD), while the other animals were maintained on the WTD without additions. Average food intake during 3 weeks of treatment as well as body weights, fat mass and lean mass at the end of treatment were unaffected by colesevelam treatment (Figure 1A-D).

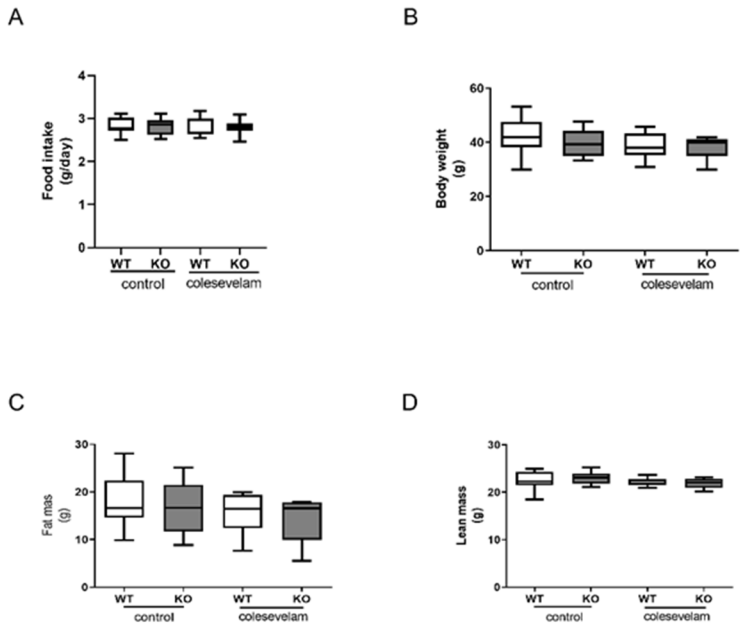

Figure 1. Colesevelam does not affect body weight in WTD-fed male Cyp2c70$^{-/-}$ mice. **(A)** Average food intake and **(B)** body weights of male Cyp2c70$^{-/-}$ mice and WT littermates on control diet and during 3 weeks of colesevelam treatment. **(C)** Fat mass and **(D)** lean mass in Cyp2c70$^{-/-}$ mice and WT littermates on control diet and after 2 weeks of colesevelam treatment as described in the materials and methods section. N = 8-9 mice/group. Data are presented as Tukey's box and whisker plots. WT: wild type; KO: Cyp2c70$^{-/-}$, WTD: Western-type diet.

3.2. Colesevelam reduces the hydrophobicity of the bile acid pool in WTD-fed Cyp2c70$^{-/-}$ mice.

Bile acid sequestration significantly increased fecal bile acid excretion in both WT and KO mice, indicating that colesevelam indeed interfered with intestinal BA absorption in these mice (Figure 2A). Next, gallbladder bile, plasma BA concentrations and composition were analyzed. As already demonstrated in our previous studies, Cyp2c70 deficiency resulted in the complete absence of hydrophilic murine-specific muricholic acids (MCAs) and high relative abundances of hydrophobic chenodeoxycholic acid (CDCA) in bile and plasma (Figure 2B, D). Consequently, the absence of Cyp2c70 caused a more hydrophobic BA pool, as indicated by a higher hydrophobicity index of biliary BA (Figure 2C). Colesevelam significantly reduced the hydrophobicity index of biliary BAs in KO mice (Figure 2C) due to a relative increase in proportion of TCA at the expense of TCDCA (Figure 2B). Interestingly, colesevelam had an opposite effect on BA hydrophobicity in WT mice because very hydrophilic TMCAs and TUDCA were relatively lower abundant in bile upon treatment and the proportion of less hydrophilic TCA increased in these mice (Figure 2C, D). Plasma total BA concentrations in KO mice remained unchanged upon colesevelam treatment (Figure 2E). In association with the reduced amounts of non 12α-hydroxylated (T)CDCA and increased proportions of 12α-hydroxylated (T)CA in KO mice treated with colesevelam, their plasma ratio of 12α-/non-12α-hydroxylated BAs was markedly increased compared to untreated KO mice (Figure 2F). Colesevelam had a similar, albeit less pronounced, effect on 12α-/non-12α-hydroxylated BA ratios in WT mice. Furthermore, to compensate the colesevelam-induced faecal BA loss, BA synthesis was stimulated. Hepatic mRNA levels of genes encoding BA synthesis enzymes Cyp7a1, considered the rate-limiting enzyme in bile acid synthesis, and Cyp8b1, controlling for CA synthesis, were significantly increased

Preprints (www.preprints.org) | NOT PEER-REVIEWED | Posted: 10 August 2023 doi:10.20944/preprints202308.0779.v1

in colesevelam-treated mice compared to untreated controls (Figure 2G). Hepatic mRNA expression of Fxr (Nr1h4) remained unchanged upon treatment, while expression of the FXR target Shp (Nr0b2) was significantly reduced in WT mice only upon colesevelam treatment (Figure 2G). Next we analyzed the mRNA levels of Fxr, Shp and Fgf15 in the terminal ileum. Fxr expression was increased in colesevelam-treated WT mice compared to untreated WT mice, but no significant changes were observed in KO mice upon colesevelam treatment. In line with the effective prevention of intestinal BA uptake, expression of the FXR downstream target genes Shp and Fgf15 was strongly reduced upon colesevelam treatment in both WT and KO mice (Figure 2H).

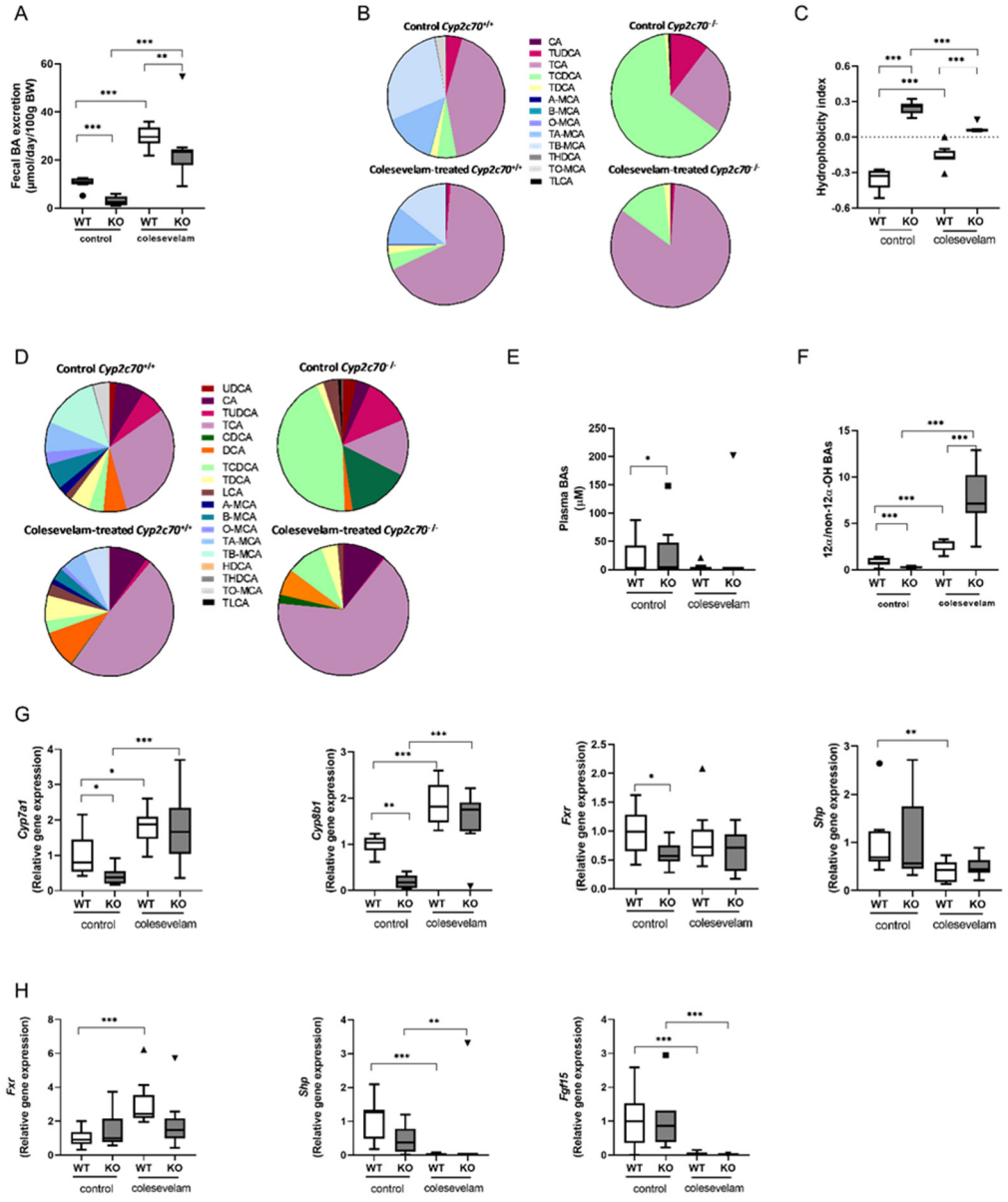

Figure 2. Colesevelam reduces the hydrophobicity of the bile acid pool in Cyp2c70$^{-/-}$ mice. **(A)** Fecal BA excretion in Cyp2c70$^{-/-}$ mice and WT littermates on control diet and after 3 weeks of colesevelam treatment. **(B)** BA composition in gallbladder bile of Cyp2c70$^{-/-}$ mice and WT littermates on control diet and after 3 weeks of colesevelam treatment. **(C)** Hydrophobicity index of biliary bile acids. **(D)** Plasma bile acid composition in Cyp2c70$^{-/-}$ mice and WT littermates on control diet and after 3 weeks of colesevelam treatment. **(E)** Total plasma BA concentrations. **(F)** Plasma ratio 12α-/non-12α-hydroxylated BAs in Cyp2c70$^{-/-}$ mice and WT littermates on control diet and after 3 weeks of colesevelam treatment. **(G)** Hepatic mRNA levels of genes involved in the BA synthesis pathway in Cyp2c70$^{-/-}$ mice and WT littermates on control diet and after 3 weeks of colesevelam treatment. **(H)**

 doi:10.20944/preprints202308.0779.v1

mRNA levels of genes involved in BA signalling in the terminal ileum of Cyp2c70$^{-/-}$ mice and WT littermates on control diet and after 3 weeks of colesevelam treatment. N = 8-9 mice/group. Data are presented as Tukey's box and whisker plots or pie charts, and p values represent *p < 0.05, **p < 0.01, and ***p < 0.001 by Kruskal-Wallis H testing followed by Conover post comparisons. WT: wild type; KO: Cyp2c70$^{-/-}$ WTD: western-type diet; CA: cholic acid; CDCA: chenodeoxycholic acid; Cyp7a1: cholesterol 7α-hydroxylase; Cyp8b1: sterol 12α-hydroxylase; Fxr: farnesoid X receptor; Shp: short heterodimer partner; Fgf15: Fibroblast growth factor 15.

3.3. Colesevelam differentially modulates WTD-induced hepatic steatosis in WT and Cyp2c70$^{-/-}$ mice.

Liver weights were unaffected by colesevelam treatment in WT and KO mice (Figure 3A). Hematoxylin and eosin (H&E) staining of liver sections revealed evidence of hepatic steatosis in WTD-fed WT mice and to a lesser extend in WTD-fed KO mice. Colesevelam treatment ameliorated hepatic steatosis in WT mice, but such an effect was not clearly discernible in KO mice (Figure 3B). Hepatic total cholesterol concentrations were significantly decreased in colesevelam-treated WT and KO mice as compared to untreated controls (Figure 3C). Hepatic phospholipid contents were unaffected by genotype and treatment (Figure 3C). While hepatic tryglyceride (TG) contents were markedly decreased in WT mice upon colesevelam treatment, BA sequestration did not further reduce the already relatively low TG accumulation in livers of KO mice (Figure 3C). Moreover, plasma concentrations of total cholesterol and triglycerides in WT and KO mice were not affected by 3 weeks of BA sequestration (Figure 3D). Surprisingly, colesevelam treatment had no impact on the hepatic mRNA levels of LDL receptor (Ldlr) (Figure 3E). Yet, there was a significant increase in the hepatic mRNA levels of the gene involved cholesterol biosynthesis (Hmgcr) in colesevelam-treated mice compared to untreated mice of both genotypes (Figure 3E), indicating that treatment with the BA sequestrant indeed induced cholesterol synthesis to provide substrate for BA production. Hepatic mRNA levels of Nr1h3 (Lxra), an important regulator of cholesterol and lipid metabolism, as well as expression levels of the lipogenic genes, Acc1 (Acaca), Fasn and Scd1 were unchanged in KO mice upon colesevelam treatment, while only Srebp1c transcript levels were significantly reduced in WT mice treated with colesevelam as compared to untreated controls (Figure 3F). Moreover, colesevelam treatment significantly increased hepatic mRNA levels of Mttp, encoding a protein involved in VLDL assembly in KO mice (Figure 3G), but it did not affect hepatic mRNA levels of Tm6sf2, a gene involved in VLDL secretion (Figure 3G). BA sequestration did not seem to affect fatty acid oxidation as expression of Ppara, Cpt1a and Acox1 remained unaffected by colesevelam treatment in WTD-fed WT as well as in KO mice (Figure 3H).

Preprints (www.preprints.org) | NOT PEER-REVIEWED | Posted: 10 August 2023 doi:10.20944/preprints202308.0779.v1

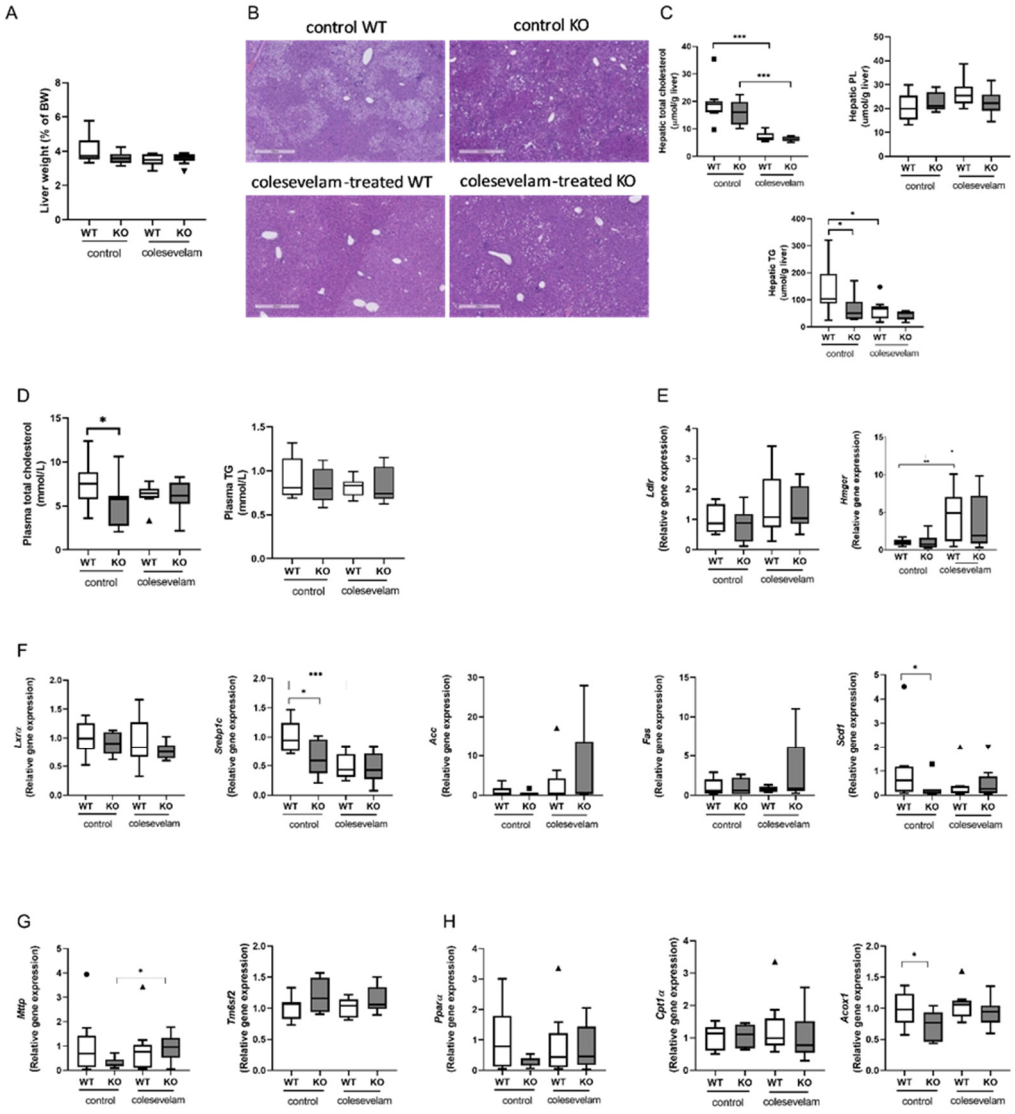

Figure 3. Colesevelam differentially modulates WTD-induced hepatic steatosis in WT and Cyp2c70$^{-/-}$ mice. **(A)** Liver weights of Cyp2c70$^{-/-}$ mice and WT littermates on control diet and after 3 weeks of colesevelam treatment. **(B)** Representative images of H&E stained liver sections of Cyp2c70$^{-/-}$ mice and WT littermates on control diet and after 3 weeks of colesevelam treatment. **(C)** Hepatic lipid contents (total cholesterol, phospholipids and triglycerides) of Cyp2c70$^{-/-}$ mice and WT littermates on control diet and after 3 weeks of colesevelam treatment. **(D)** Plasma total cholesterol and triglycerides of Cyp2c70$^{-/-}$ mice and WT littermates on control diet and after 3 weeks of colesevelam treatment. **(E)** Hepatic mRNA levels of genes involved in LDL uptake (Ldlr) and cholesterol biosynthesis (Hmgcr) in Cyp2c70$^{-/-}$ mice and WT littermates on control diet and after 3 weeks of colesevelam treatment. **(F)** Hepatic mRNA levels of genes involved in lipogenesis in Cyp2c70$^{-/-}$ mice and WT littermates on control diet and after 3 weeks of colesevelam treatment. **(G)** Hepatic mRNA levels of genes involved in VLDL assembly and secretion in Cyp2c70$^{-/-}$ mice and WT littermates on control diet and after 3 weeks of colesevelam treatment. **(H)** Hepatic mRNA levels of genes involved in in fatty acid oxidation (Pparα, Cpt1α, Acox1) in Cyp2c70$^{-/-}$ mice and WT littermates on control diet and after 3 weeks of colesevelam treatment. N = 8-9 mice/group. Quantitative data are presented as Tukey's box-and-whisker plots and p values represent *$p < 0.05$, and ***$p< 0.001$ by Kruskal-Wallis H testing followed by Conover post comparisons. PL: phospholipids; TG: triglycerides; Ldlr: low density lipoprotein receptor; Hmgcr: 3-hydroxy-3-methyl-glutaryl-coenzyme A reductase; Lxrα: liver X receptor alpha; Srebp1c: sterol regulatory element binding protein 1c; Acc: Acetyl-CoA carboxylase (Acaca); Fasn:fatty acid synthase; Scd1: acyl-CoA desaturase 1; Mttp: microsomal triglyceride transfer protein;

 doi:10.20944/preprints202308.0779.v1

Tm6sf2: transmembrane 6 superfamily member 2; Pparα:peroxisome proliferator-activated receptor alpha; Cpt1α: carnitine palmitoyltransferase 1A; Acox1: acyl-Coenzyme A oxidase 1.

3.4. Colesevelam ameliorates liver damage in WTD-fed Cyp2c70$^{-/-}$ mice.

Liver damage markers AST and ALT in plasma of WTD-fed KO mice that did not receive colesevelam treatment were significantly higher than in WT littermates. Importantly, 3 weeks of colesevelam treatment fully normalized ALT and AST levels in KO mice (Figure 4A). Next, liver sections were stained with Sirius Red to visualize collagen deposition. In accordance with our previous findings, livers of untreated WTD-fed KO mice showed moderately increased collagen deposition compared to their WT littermates, which was mainly localized in the periportal areas. However, considerable variation in the degree of fibrosis was observed within the group of untreated KO mice (Figure 4B). Three weeks of treatment with colesevelam did not translate into a significant reduction of the collagen-stained areas in livers of KO mice (Figure 4B). Interestingly, hepatic mRNA levels of genes involved in fibrogenesis were elevated in untreated KO mice compared to WT and markedly upon colesevelam treatment (Figure 4C), suggesting that changes in fibrogenesis are apparent, but that these have not yet translated into detectable differences in the amounts of deposited collagen in the livers of KO mice within the 3-week time frame of treatment that was applied. Moreover, expression of monocyte chemoattractant protein-1 (Mcp1, Ccl2) was significantly decreased in colesevelam-treated KO mice as compared to untreated KO mice (Figure 4D). However, hepatic expression of the macrophage marker F4/80 (Adgre1) did not differ between any of the groups. Additionally, expression of the marker of cellular senescence P16 (cdkn2a) was significantly increased in untreated KO mice as compared to WT but was not decreased upon colesevelam treatment (Figure 4D). CK19 immuno-staining of liver sections revealed a significant increase in the number of cholangiocytes in livers of untreated WTD-fed KO mice compared to WT controls. However, the reduction of the amount of cholangiocytes in livers that was achieved by 3 weeks of colesevelam treatment in KO mice did not reach statistical significance (Figure 4E).

Preprints (www.preprints.org) | NOT PEER-REVIEWED | Posted: 10 August 2023 doi:10.20944/preprints202308.0779.v1

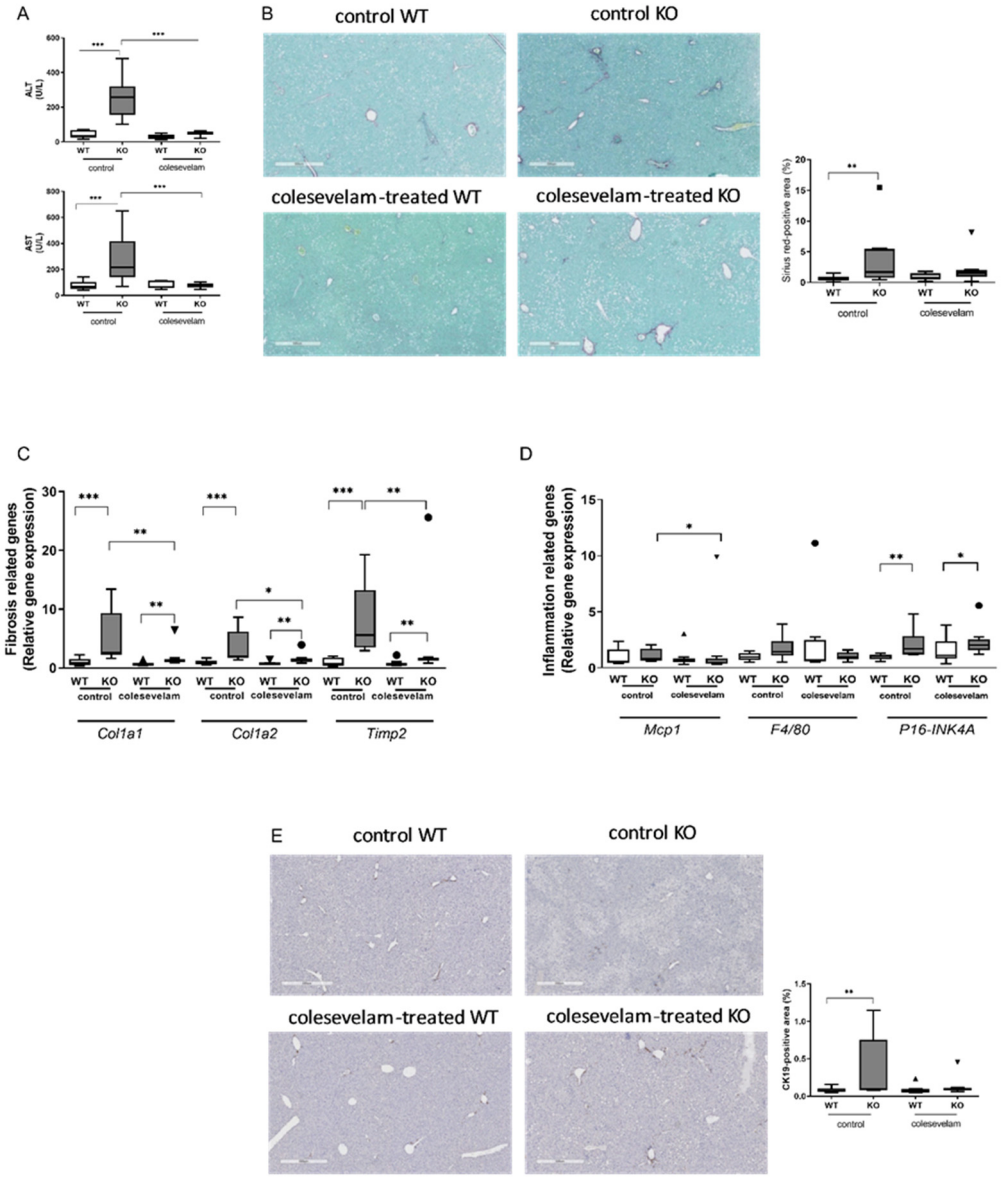

Figure 4. Colesevelam ameliorates liver damage in WTD-fed Cyp2c70$^{-/-}$ mice. **(A)** Levels of the liver damage markers aminotransferase and alanine aminotransferase in plasma of Cyp2c70$^{-/-}$ mice and WT littermates on control diet and after 3 weeks of colesevelam treatment. **(B)** Representative images of SiriusRed Fast Green-stained liver sections and quantification of SiriusRed-positive areas of Cyp2c70$^{-/-}$ mice and WT littermates on control diet and after 3 weeks of colesevelam treatment. **(C)** Hepatic mRNA levels of genes involved in fibrogenesis in Cyp2c70$^{-/-}$ mice and WT littermates on control diet and after 3 weeks of colesevelam treatment. **(D)** Hepatic mRNA levels of genes involved in inflammation and cellular senescence in Cyp2c70$^{-/-}$ mice and WT littermates on control diet and after 3 weeks of colesevelam treatment. **(E)** Representative images of liver sections stained for the cholangiocyte marker CK19 and quantification of CK19-positive areas in Cyp2c70$^{-/-}$ mice and WT littermates on control diet and after 3 weeks of colesevelam treatment. N = 8-9 mice/group. Quantitative data are presented as Tukey's box-and-whisker plots and p values represent *$p < 0.05$, **$p < 0.01$, and ***$p < 0.001$ by Kruskal-Wallis H testing followed by Conover post comparisons. ALT: alanine transaminase; AST: aspartate aminotransferase; CK19: cytokeratin 19; Col1a1: collagen type I alpha 1 chain; Col1a2: collagen type I alpha 2 chain; Timp2: metalloproteinase inhibitor 2; Mcp1: monocyte chemoattractant protein 1; F4/80: EGF-like module containing mucin-like hormone receptor-like 1 (Emr1); P16-INK4A: cyclin-dependent kinase inhibitor 2A, (Cdkn2a).

Preprints (www.preprints.org) | NOT PEER-REVIEWED | Posted: 10 August 2023 doi:10.20944/preprints202308.0779.v1

3.5. Colesevelam modulates the absorption efficiency of dietary energy in WTD-fed WT and Cyp2c70$^{-/-}$ mice.

Fecal excretion of neutral sterols (cholesterol and its bacterial derivatives) was increased in untreated WTD-fed KO mice compared to WT controls, which is in line with previous observations [22]. Interestingly, colesevelam treatment induced an increased excretion of fecal neutral sterols in WT mice, whereas such an effect was not discernible upon treatment of KO mice (Figure 5A). In addition, colesevelam-treated WT and KO mice lost more energy in the feces as compared to their untreated controls due to a reduced absorption efficiency of dietary energy (Figure 5B, C).

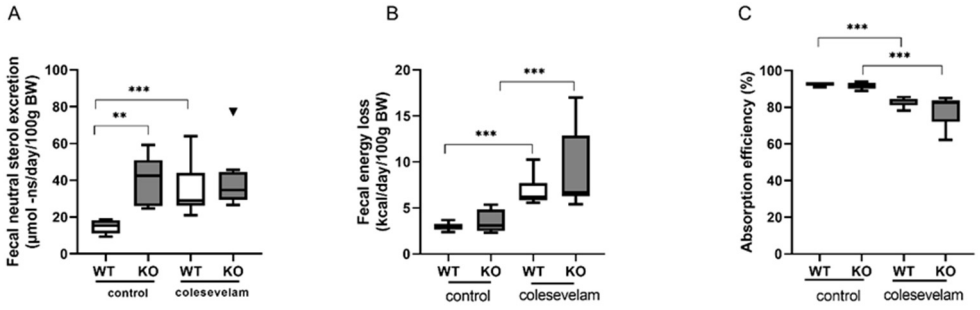

Figure 5. Colesevelam modulates the absorption efficiency of dietary energy in WTD-fed WT and Cyp2c70$^{-/-}$ mice. **(A)** Fecal neutral sterol excretion in Cyp2c70$^{-/-}$ mice and WT littermates on control diet and after 3 weeks of colesevelam treatment. **(B)** Fecal energy content in Cyp2c70$^{-/-}$ mice and WT littermates on control diet and after 3 weeks of colesevelam treatment. **(C)** Absorption efficiency (%) calculated as described in the materials and methods section. N = 8-9 mice/group. Data are presented as Tukey's box-and-whisker plots and p values represent **$p < 0.01$, and ***$p < 0.001$ by Kruskal-Wallis H testing followed by Conover post comparisons. NS: neutral sterol.

3.6. Colesevelam does not affect glucose excursions and insulin sensitivity in WTD-fed Cyp2c70$^{-/-}$ mice upon 2 weeks of treatment.

To evaluate the effects of bile acid sequestration by colesevelam on glucose metabolism and insulin sensitivity, fasting blood glucose and plasma insulin concentrations were determined after two weeks of treatment. Fasting glucose and fasting insulin levels did, however, not differ significantly between any of the groups (Figure 6A). The HOMA-IR was significantly lower in untreated WTD-fed KO as compared to WT controls but was not significantly affected by colesevelam treatment in WT and in KO mice (Figure 6A). Moreover, bile acid sequestration had no significant effects on blood glucose excursions, nor on plasma insulin levels in WT and KO mice during an OGTT (Figure 6B).

Preprints (www.preprints.org) | NOT PEER-REVIEWED | Posted: 10 August 2023 doi:10.20944/preprints202308.0779.v1

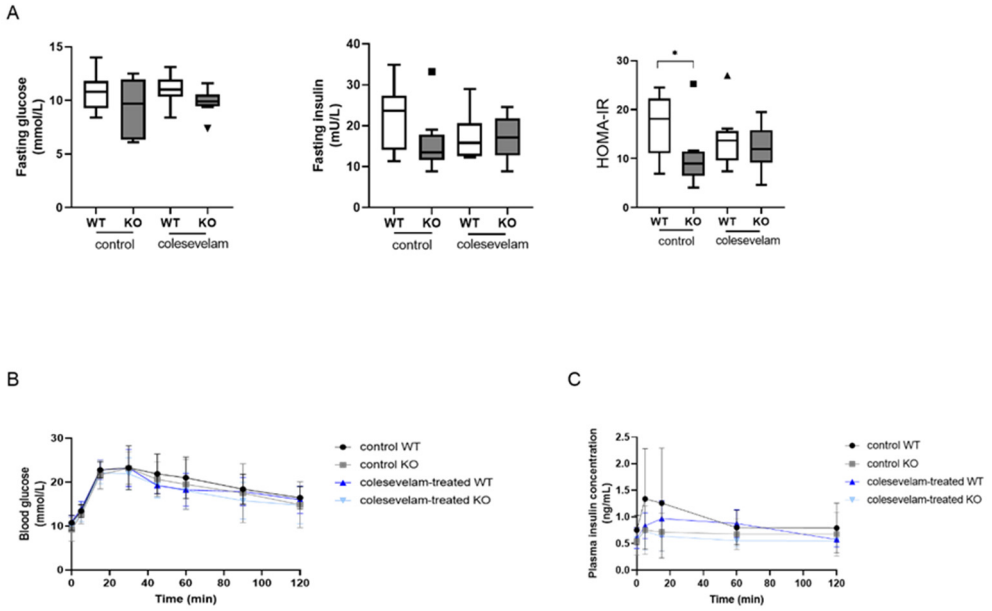

Figure 6. Colesevelam does not affect insulin sensitivity in WTD fed-Cyp2c70$^{-/-}$ mice upon 2 weeks of treatment. **(A)** Fasting blood glucose and plasma insulin levels, as well as HOMA-IR in Cyp2c70$^{-/-}$ mice and WT littermates on control diet and after 2 weeks of colesevelam treatment. **(B)** Blood glucose concentrations in Cyp2c70$^{-/-}$ mice and WT littermates during OGTT performed with or without colesevelam treatment for 2 weeks. **(C)** Insulin concentrations in Cyp2c70$^{-/-}$ mice and WT littermates during OGTT performed with or without colesevelam treatment for 2 weeks. N = 8-9 mice/group. Data are presented as mean ± SD and p values represent *p < 0.05 by Mann-Whitney U non parametric comparisons. HOMA-IR: homeostatic model assessment of insulin resistance; OGTT: oral glucose tolerance test.

4. Discussion

In this study, we show that bile acid sequestration by colesevelam increases the proportion of 12α-hydroxylated BAs in the circulating bile acid pool, thereby differentially affecting its hydrophobicity in WT and *Cyp2c70*-deficient mice. Whereas BA sequestration increases the hydrophobicity of biliary BAs in WT mice, it causes a substantial decrease of BA hydrophobicity bile in KO mice. Moreover, our findings provide evidence that colesevelam alleviates hepatic injury in WTD-fed *Cyp2c70*$^{-/-}$ mice without affecting insulin sensitivity in these mice with a human-like bile acid metabolism. As previously reported by us [19,29] and others [20,21] *Cyp2c70*$^{-/-}$ mice have a human-like bile acid composition, lacking the hydrophilic and hepatoprotective mouse/rat-specific MCA species and showing high abundances of hydrophobic and cytotoxic CDCA in their circulating BA pool. The altered BA composition in *Cyp2c70*$^{-/-}$ mice is associated with the development of cholangiopathy and liver fibrosis [19]. We hypothesize that the beneficial effects of colesevelam on liver pathology in KO mice might be mediated at least in part by a shift in BA production towards more 12α-hydroxylated CA and less CDCA due to increased activity of sterol 12α-hydroxylase in the levers of these mice, resulting in a more hydrophilic, less cytotoxic BA composition in mice lacking *Cyp2c70*. In line with the increased 12α-/non-12α-hydroxylated BA ratio in KO mice following colesevelam treatment, these mice showed a strongly upregulated hepatic mRNA expression of *Cyp8b1*, encoding sterol 12α-hydroxylase. While this manuscript was in preparation, Truong et al. reported that interrupting the enterohepatic circulation of BAs by pharmacological inhibition of the ileal BA transporter (IBAT/ASBT/SLC10A2) improves cholangiopathy in *Cyp2c70*$^{-/-}$ mice [30]. Although the results of that study largely support our conclusions, some differences between the study of Truong et al. and our current study do exist. First of all, Truong and colleagues started their intervention in mice at the age of only 4 weeks and was continued for 8 weeks. As we have previously

shown [19], *Cyp2c70*$^{-/-}$ do have increased plasma transaminases, indicative of hepatocyte damage, at the age of 3 weeks but do not yet display an increase in hepatic fibrosis. Therefore, with respect to liver fibrosis, the ASBT inhibition as applied by Truong in all likelihood prevented collagen deposition rather than restoring pre-existing fibrosis. In our current study, mice received the colesevelam treatment starting at the age of 20-22 weeks, thus at an age when fibrosis is already eminent. Furthermore, in the current study we only applied BA sequestration for 3 weeks, a duration that is considerably shorter as compared to the 8 weeks of ASBT inhibition applied by Truong and colleagues. Another difference between our study and the study of Truong is the diet that was given to the mice during the intervention. In the study by Truong and co-workers, the mice were fed a regular chow diet, whereas we fed the mice a WTD in this study in order to explore the metabolic effects of BA sequestration in mice with a human-like BA composition. As male mice are more prone to develop obesity and insulin resistance upon WTD feeding, only male mice were used in our current study. Male *Cyp2c70*$^{-/-}$ mice do, however, display less severe liver pathology compared to females [19,30]. Importantly, disruption of the enterohepatic circulation of BAs by ASBT inhibition might exert other effects than when using BA sequestrants. BA sequestrants like colesevelam bind BAs in the intestine, preventing their re-absorption and removing them from the enterohepatic circulation, whereas pharmacological ASBT inhibition prevents BA re-absorption by blocking the enterocytic uptake transporter, leading to increased amounts of free BAs entering the colon, where they can be deconjugated and converted into secondary species by the bacteria that are populating the colon and subsequently be absorbed by passive diffusion. In line, Truong and co-workers reported a substantial increase in the proportion of TDCA in livers of *Cyp2c70*$^{-/-}$ mice upon ASBT inhibition, leading to an increased BA hydrophobicity despite increased 12α-/non-12α-hydroxylated BA ratios. We did not observe such an increase in the proportion TDCA in bile, but colesevelam treatment did elicit an increase in the 12α-/non-12α-hydroxylated BA ratios, resulting in a considerably reduced hydrophobicity of biliary BAs. Intriguingly, despite the increased BA hydrophobicity in their study, Truong and colleagues did observe robust hepatoprotective effects in *Cyp2c70*$^{-/-}$ upon ASBT inhibition, which were attributed to decreased hepatic total BA concentrations. It is however not clear to what extend the reduced total BA concentrations reflect lower BA concentrations within the hepatocytes or whether they reflect an altered contribution BAs present within the biliary tree in that study. Colesevelam treatment reduced absorption efficiency of energy from the diet in WT as well as in KO mice. Surprisingly, this did not translate into lower body weights or decreased adiposity of the mice. We hypothesize that the colesevelam-induced reduction in hydrophobicity BA pool would lead to reduced activation of TGR5 in brown adipose tissue (BAT), because more hydrophobic BAs are potent ligands for this receptor. Reduced TGR5 activation would, thus, lead to a reduced amount of energy that is used for thermogenesis. Energy expenditure and body temperature were not measured in the current study, but we did analyze the mRNA levels of the thermogenic genes *Ucp1* and *Dio2* in BAT. The expression levels of both of these genes were similar in all groups (Supplementary Figure 1), suggesting that *Cyp2c70* deficiency as well as the altered BA composition upon colesevelam treatment in these KO mice and their WT littermates did not impact TGR5 signalling or thermogenesis. The BA receptor FXR is known to regulate glucose metabolism [2] and the FXR agonist OCA, an analogue of CDCA, has been demonstrated to improve insulin sensitivity in patients with type 2 diabetes mellitus [31]. Furthermore, we have previously shown that 2 weeks of colesevelam treatment increases the metabolic clearance rate of glucose in diabetic *db*/*db* mice by improving insulin sensitivity in peripheral tissues [16] and also that CDCA may improve skeletal muscle insulin sensitivity [32]. Therefore, we investigated the effects of colesevelam treatment on glucose metabolism in mice in the context of a human-like BA composition, i.e., in *Cyp2c70*$^{-/-}$ mice. KO mice had a lower HOMA-IR compared to their WT littermates, but 2 weeks of colesevelam treatment had no effects on HOMA-IR in both KO and WT mice and did not impact glucose excursions and plasma insulin levels during an OGTT. Together, these data indicate that, in contrast to previous the observations in *db*/*db* mice [16], colesevelam did not impact insulin sensitivity in WTD-fed *Cyp2c70*$^{-/-}$ mice and in their WT littermates. As insulin resistance in *db*/*db* mice is much more extreme than in WTD-fed C57BL/6J mice, it may be interesting to study the effects of colesevelam in

mice with a human-like BA composition in the context of a more severe insulin resistant phenotype at the start of the intervention.

5. Conclusions

In conclusion, bile acid sequestration with colesevelam improved liver pathology in *Cyp2c70*$^{-/-}$ mice. The improvement was associated with a reduced hydrophobicity of biliary BAs in *Cyp2c70*$^{-/-}$ mice. However, 2 weeks of BA sequestration had no effects on insulin sensitivity in WTD-fed *Cyp2c70*$^{-/-}$ mice.

Supplementary Materials: The following supporting information can be downloaded at the website of this paper posted on Preprints.org. Figure S1: Colesevelam does not impact the expression of genes involved in thermogenesis in brown adipose tissue of WTD fed-WT and *Cyp2c70*$^{-/-}$ mice.

Author Contributions: Conceptualization, Jan Freark De Boer and Folkert Kuipers; Formal analysis, Anna Palmiotti, Theo Van Dijk and Vincent W. Bloks; Funding acquisition, Henkjan Verkade, Jan Freark De Boer and Folkert Kuipers; Investigation, Anna Palmiotti, Hilde D. De Vries, Milaine V. Hovingh, Martijn Koehorst, Niels L. Mulder, Esther Verkade, Melany K. Veentjer and Rick Havinga; Supervision, Henkjan Verkade, Jan Freark De Boer and Folkert Kuipers; Writing – original draft, Anna Palmiotti; Writing – review & editing, Henkjan Verkade, Jan Freark De Boer and Folkert Kuipers. All authors have read and agreed to the published version of the manuscript.

Funding: A.P. is supported by the European Union's Horizon 2020 research and innovation programme under the Marie Skłodowska-Curie grant agreement (No.754425). H.D.d.V. is supported by the PhD program of Campus Fryslân, University of Groningen and Medical Center Leeuwarden. J.F.d.B. is supported by the Nutrition & Health initiative of the University of Groningen. F.K. is supported by an unrestricted grant from the Noaber Foundation, Lunteren, The Netherlands.

Institutional Review Board Statement: All animal experiments were approved by the Dutch Central Committee for Animal Experiments and the Animal Welfare Body of the University of Groningen (Dutch National Central Commission for Animal Experiments, CCD, license number AVD10500202115290).

Data Availability Statement: All data are in this manuscript.

Conflicts of Interest: The authors declare no conflict of interest.

References

1. Yang, A. Palmiotti, and F. Kuipers, Emerging roles of bile acids in control of intestinal functions, CurrOpin Clin NutrMetab Care, vol. 24, no. 2, pp. 127–133, 2021, doi: 10.1097/MCO.0000000000000709.
2. F. Kuipers, V. W. Bloks, and A. K. Groen, Beyond intestinal soap—bile acids in metabolic control, Nat Rev Endocrinol, vol. 10, no. 8, pp. 488–498, Aug. 2014, doi: 10.1038/nrendo.2014.60.
3. A. Floreani and C. Mangini, Primary biliary cholangitis: Old and novel therapy, Eur J Intern Med, vol. 47, pp. 1–5, Jan. 2018, doi: 10.1016/j.ejim.2017.06.020.
4. L. Verbeke et al., FXR agonist obeticholic acid reduces hepatic inflammation and fibrosis in a rat model of toxic cirrhosis, Nature Publishing Group, 2016, doi: 10.1038/srep33453.
5. Y. Y. Fan, W. Ding, C. Zhang, L. Fu, D. X. Xu, and X. Chen, Obeticholic acid prevents carbon tetrachloride-induced liver fibrosis through interaction between farnesoid X receptor and Smad3, Int Immunopharmacol, vol. 77, p. 105911, Dec. 2019, doi: 10.1016/J.INTIMP.2019.105911.
6. K. v. Kowdleyet al., A randomized, placebo-controlled, phase II study of obeticholic acid for primary sclerosing cholangitis, J Hepatol, vol. 73, no. 1, pp. 94–101, Jul. 2020, doi: 10.1016/J.JHEP.2020.02.033.
7. F. Nevenset al., A Placebo-Controlled Trial of Obeticholic Acid in Primary Biliary Cholangitis, New England Journal of Medicine, vol. 375, no. 7, pp. 631–643, Aug. 2016, doi: 10.1056/nejmoa1509840.
8. V. Manne and K. v. Kowdley, Obeticholic acid in primary biliary cholangitis: where we stand, CurrOpin Gastroenterol, vol. 35, no. 3, pp. 191–196, May 2019, doi: 10.1097/MOG.0000000000000525.
9. C. L. Bowlus, Obeticholic acid for the treatment of primary biliary cholangitis in adult patients: clinical utility and patient selection, Hepat Med, vol. 8, pp. 89–95, 2016, doi: 10.2147/HMER.S91709.
10. B. Zhang, F. Kuipers, J. F. de Boer, and J. A. Kuivenhoven, Modulation of bile acid metabolism to improve plasma lipid and lipoprotein profiles, J Clin Med, vol. 11, no. 1, Jan. 2022, doi: 10.3390/jcm11010004.

11. D. Fuchs et al., Colesevelam attenuates cholestatic liver and bile duct injury in Mdr2 −/− mice by modulating composition, signalling and excretion of faecal bile acids, Gut, vol. 67, pp. 1683–1691, 2018, doi: 10.1136/gutjnl-2017-314553.
12. A. Baghdasaryan et al., Inhibition of intestinal bile acid absorption improves cholestatic liver and bile duct injury in a mouse model of sclerosing cholangitis, J Hepatol, vol. 64, no. 3, pp. 674–681, Mar. 2016, doi: 10.1016/J.JHEP.2015.10.024.
13. H. E. Bays, R. B. Goldberg, K. E. Truitt, and M. R. Jones, Colesevelam Hydrochloride Therapy in Patients With Type 2 Diabetes Mellitus Treated With Metformin Glucose and Lipid Effects. [Online]. Available: https://jamanetwork.com/
14. F. J. Zieve, M. F. Kalin, S. L. Schwartz, M. R. Jones, and W. L. Bailey, Results of the glucose-lowering effect of WelChol study (GLOWS): A randomized, double-blind, placebo-controlled pilot study evaluating the effect of Colesevelam hydrochloride on glycemic control in subjects with type 2 diabetes, Clin Ther, vol. 29, no. 1, pp. 74–83, Jan. 2007, doi: 10.1016/j.clinthera.2007.01.003.
15. G. Brufauet al., Improved Glycemic Control with Colesevelam Treatment in Patients with Type 2 Diabetes Is Not Directly Associated with Changes in Bile Acid Metabolism, HEPATOLOGY, vol. 52, pp. 1455–1464, 2010, doi: 10.1002/hep.23831.
16. M. Meissner, H. Herrema, T. H. van Dijk, A. Gerding, and R. Havinga, Bile Acid Sequestration Reduces Plasma Glucose Levels in db/db Mice by Increasing Its Metabolic Clearance Rate, PLoS One, vol. 6, no. 11, p. 24564, 2011, doi: 10.1371/journal.pone.0024564.
17. U. Beil, J. R. Crouse, K. Einarsson, and S. M. Grundy, Effects of interruption of the enterohepatic circulation of bile acids on the transport of very low density-lipoprotein triglycerides, Metabolism, vol. 31, no. 5, pp. 438–444, May 1982, doi: 10.1016/0026-0495(82)90231-1.
18. J. R. Crouse, Hypertriglyceridemia: A contraindication to the use of bile acid binding resins, Am J Med, vol. 83, no. 2, pp. 243–248, Aug. 1987, doi: 10.1016/0002-9343(87)90692-9.
19. J. F. de Boer et al., Cholangiopathy and Biliary Fibrosis in Cyp2c70-Deficient Mice Are Fully Reversed by Ursodeoxycholic Acid, CMGH, vol. 11, no. 4, pp. 1045–1069, Jan. 2021, doi: 10.1016/J.JCMGH.2020.12.004.
20. A. Honda et al., Regulation of bile acid metabolism in mouse models with hydrophobic bile acid composition, J Lipid Res, vol. 61, no. 1, pp. 54–69, 2020, doi: 10.1194/JLR.RA119000395.
21. S. Straniero, A. Laskar, C. Savva, J. Härdfeldt, B. Angelin, and M. Rudling, Of mice and men: Murine bile acids explain species differences in the regulation of bile acid and cholesterol metabolism, J Lipid Res, vol. 61, no. 4, pp. 480–491, Apr. 2020, doi: 10.1194/JLR.RA119000307.
22. R. Li et al., Low production of 12α-hydroxylated bile acids prevents hepatic steatosis in Cyp2c70-/- mice by reducing fat absorption, J Lipid Res, vol. 62, 2021, doi: 10.1016/J.JLR.2021.100134.
23. M. B. Dommerholtet al., Short-term protein restriction at advanced age stimulates FGF21 signalling, energy expenditure and browning of white adipose tissue, FEBS Journal, vol. 288, no. 7, pp. 2257–2277, Apr. 2021, doi: 10.1111/FEBS.15604.
24. T. H. van Dijk et al., A novel approach to monitor glucose metabolism using stable isotopically labelled glucose in longitudinal studies in mice, Lab Anim, vol. 47, no. 2, pp. 79–88, Apr. 2013, doi: 10.1177/0023677212473714/ASSET/IMAGES/LARGE/10.1177_0023677212473714-FIG2.JPEG.
25. H. M. Egginket al., Chronic infusion of taurolithocholate into the brain increases fat oxidation in mice, Journal of Endocrinology, vol. 236, no. 2, pp. 85–97, Feb. 2018, doi: 10.1530/JOE-17-0503.
26. Canadian Journal of Biochemistry and Physiology Issued by THE NATIONAL RESEARCH COUNCIL OF CANADA A RAPID METHOD OF TOTAL LIPID EXTRACTION AND PURIFICATION.
27. O. A. H. O. Ronda, T. H. van Dijk, H. J. Verkade, and A. K. Groen, Measurement of Intestinal and Peripheral Cholesterol Fluxes by a Dual-Tracer Balance Method, CurrProtoc Mouse Biol, vol. 6, no. 4, pp. 408–434, Dec. 2016, doi: 10.1002/CPMO.16.
28. D. Stricker, BrightStat.com: Free statistics online, Comput Methods Programs Biomed, vol. 92, no. 1, pp. 135–143, Oct. 2008, doi: 10.1016/J.CMPB.2008.06.010.
29. J. F. de Boer et al., A human-like bile acid pool induced by deletion of hepatic Cyp2c70 modulates effects of FXR activation in mice, J Lipid Res, vol. 61, no. 3, pp. 291–305, 2020, doi: 10.1194/JLR.RA119000243.
30. J. K. Truong et al., Ileal bile acid transporter inhibition in Cyp2c70 KO mice ameliorates cholestatic liver injury, J Lipid Res, vol. 63, no. 9, p. 100261, Sep. 2022, doi: 10.1016/J.JLR.2022.100261.

31. S. Mudaliar et al., Efficacy and safety of the farnesoid x receptor agonist Obeticholic acid in patients with type 2 diabetes and non-alcoholic fatty liver disease, Gastroenterology, vol. 145, no. 3, pp. 574-582.e1, Sep. 2013, doi: 10.1053/j.gastro.2013.05.042.
32. S. Zhong et al., Haploinsufficiency of CYP8B1 associates with increased insulin sensitivity in humans, J Clin Invest, vol. 132, no. 21, Nov. 2022, doi: 10.1172/JCI152961.